Explicit Design Formulas for Waveguide Single-Sided Filters

J. DAVID RHODES, MEMBER, IEEE

Abstract—Explicit formulas are given for the design of optimum single-sided waveguide filters. Using a uniform waveguide with iris-coupled series stubs irregularly spaced along the waveguide, this class of filter results in a significant reduction in the number of resonators required to meet single-passband and single-stopband specifications over conventional techniques. Design information is given for both the Chebyshev and elliptic function cases from which the required structure may be obtained without recourse to synthesis procedures.

Computer simulations of the response characteristics of both the quarter- and modified three-quarter-wave coupled quasi low-pass and the quasi high-pass designs are given. Experimental results on fifth-degree Chebyshev filters operating in X band for the former case are presented showing close agreement with theory.

I. INTRODUCTION

IN MANY microwave systems it is necessary to attenuate a single prescribed frequency band while maintaining a minimum level of attenuation in one other prescribed band. For this single-sided type of specification it is advantageous to design the required filter to possess an asymmetric response characteristic For example, consider the specification:

Passband

9.000 → 9.200 GHz
Return loss > 25 dB.

Stopband

9.210 → 9.410 GHz
Insertion loss > 65 dB.

Using a conventional direct-coupled cavity waveguide filter designed on a Chebyshev basis, 21 cavities are required to meet this specification [1]. A similar result holds for the symmetrical bandstop filter design from a Chebyshev prototype [2]. For the optimum symmetrical bandstop filter based upon an elliptic function response [3], 11 resonators are needed. However, using the single-sided type of filters presented in this paper, a degree-13 filter is necessary when the Chebyshev prototype is used but only 8 resonators are required in the optimum elliptic function design.

Initially, after presenting a section related to the design equations, the modified asymmetric prototype network exhibiting a Chebyshev characteristic is derived with explicit formulas for the element values. The frequency transformation which maps the stopband into a narrow-frequency band is then considered and appropriate parameters are defined which enable the design engineer to determine the required degree to meet a given specification. A similar treatment is then developed for the optimum elliptic function response with explicit formulas for element values in the modified "natural prototype" [4]. Again, auxiliary parameters are defined in order to readily determine the degree of the required filter.

The physical structure which is used to realize these single-sided types of characteristics is the uniform waveguide with iris-coupled series stubs which are accurately spaced at prescribed unequal distances along the guide. The exact distances are obtainable immediately from the prototype network and the 3-dB (or 20-dB) bandwidth of the resonators is also obtained explicitly. This design information enables use to be made of any type of series resonator. For the inductive iris-coupled rectangular resonator, the coupling susceptance and electrical length of the cavity may be obtained in the usual manner using an iterative technique [2], [3].

For the quasi low-pass design, the stubs spacings are either between zero and a quarter of a wavelength long at the operating frequency or between one half and three quarters of a wavelength long. In the former case, even if alternate stubs are located on opposite sides of the main guide it may be physically impossible to provide the correct separation. Furthermore, problems can arise with the evanescent mode interaction [2]. Thus the additional half wavelength of separation may be required. However, this will restrict the bandwidth of the passband. Intuitively, this may readily be appreciated if one considers the symmetrical bandstop filter designed on a Chebyshev basis where the stub separation is exactly three quarters of a wavelength at the center of the stopband. If one now considers a lower frequency at which the electrical spacings are one half of a wavelength, then the total attenuation becomes the sum of the individual attenuations of each stub which, for a filter with a stopband of the order of 100 MHz, at 10 GHz could result in several decibels of attenuation. For the specification quoted above this would not be important but for a true quasi low-pass specification this would not be acceptable.

It is possible to provide three stepped impedance lines between each stub [2] to overcome this problem. However, it is shown in this paper that the introduction of a small

Manuscript received August 23, 1974; revised February 7, 1975.
The author is with the Department of Electrical and Electronic Engineering, University of Leeds, Leeds LS2 9JT, England.

capacitive discontinuity beneath the stub is also a successful process and allows the significant economical advantage of using a uniform waveguide to be retained. It is shown that by deriving the lattice section for each element in this filter only trivial modifications to the resonant frequencies and electrical separations of the stubs are required.

The quasi high-pass design possess stub separations which are between one quarter and one half of a wavelength long at the transition frequency. This structure provides an adequate passband bandwidth for most applications and no further modifications are required.

Finally, results on an experimental filter based upon a fifth-degree Chebyshev prototype in WR90 are given. This quasi low-pass design uses stub separations between one half and three quarters of a wavelength long and the two cases with and without capacitive discontinuity compensation are presented. The results show excellent agreement with the theoretical characteristics.

II. EXPLICIT DESIGN FORMULAS

The physical structure for the filter is depicted in Fig. 1 and is defined by the resonant wavelengths of the stubs, their 3-dB bandwidths, and electrical separations. Furthermore, in the quasi low-pass design where capacitive compensation is required in the three quarter wavelength coupled stub case, the susceptance of the capacitive discontinuity is also required.

The initial specifications which are required are shown in Fig. 2(a) and (b) for the quasi low-pass and quasi high-pass cases. These are as follows:

- λ_{g2} stopband upper cutoff wavelength
- λ_{g1} stopband lower cutoff wavelength
- λ_{gp} passband edge wavelength
- L_A stopband insertion loss (in decibels)
- L_R passband return loss (in decibels).

A. Quasi Low-Pass (Stub Separation $< \lambda_{gp}/4$*)*

1) Chebyshev Design:

Compute

$$x = \frac{\lambda_{gp} - \lambda_{g1}}{\lambda_{g1} - \lambda_{g2}}.$$

Noting that

$$y = (1 + c)\{\tfrac{1}{2} + x + [x(1 + x)]^{1/2}\}$$

where

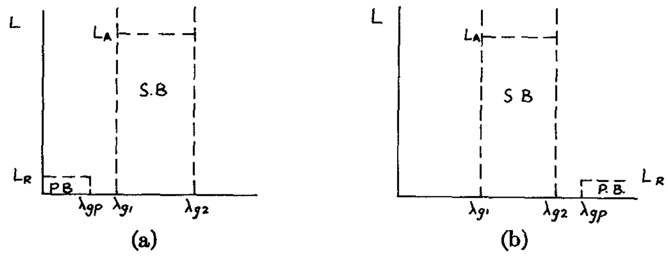

Fig. 2. Basic specifications. (a) Quasi low pass. (b) Quasi high pass.

$$c = \cos\left[\frac{\pi}{2n}\right]$$

determine the minimum value of n with the aid of

$$n > \frac{L_A + L_R}{20 \log [y + (y^2 - 1)^{1/2}]}$$

with the initial estimate $c = 1$.

Compute η from

$$\eta = \sinh\left[\frac{1}{n}\cosh^{-1}\left(10 \uparrow \left(\frac{L_R}{20}\right)\right)\right]$$

then the resonant frequency of all of the stubs occurs at

$$\lambda_{g0} = \lambda_{g1} - (\lambda_{gp} - \lambda_{g1})\left(\frac{1 + c}{y - 1}\right)$$

the 3-dB bandwidths are given by

$$\Delta\lambda_{gr} = \frac{2 \sin [(2r - 1)\pi/2n](y + c)(1 + c)}{\eta(y - 1)} (\lambda_{g1} - \lambda_{g0}), \qquad r = 1 \rightarrow n$$

and the phase separation of the stubs by

$$\psi_{r,r+1}|_{\lambda_g = \lambda_{gp}} = \tan^{-1}\left[\frac{\eta}{\sin [r\pi/n]}\right], \qquad r = 1 \rightarrow n - 1$$

with $0 < \psi_{r,r+1} < \pi/2$.

2) Optimum Elliptic Function Design:[1]

Compute

$$x = \frac{\lambda_{gp} - \lambda_{g1}}{\lambda_{g1} - \lambda_{g2}}.$$

Noting that

$$m^{-1/2} = \frac{1 + (1 + c)x + [1 + 4(1 + c)^2 x + 4(1 + c)^2 x^2]^{1/2}}{2}$$

with

$$c = cd[K/n]$$

and determine n with the aid of [3]

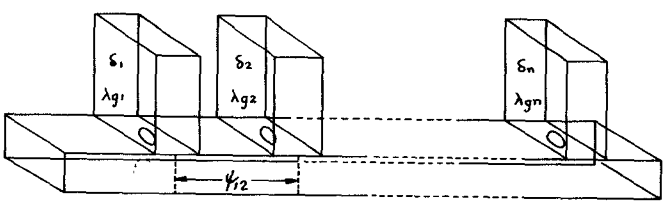

Fig. 1. The single-sided waveguide filter.

[1] Jacobian elliptic functions are used throughout with the usual rotation, e.g., [4].

$$13.65 \frac{nK'}{K} > L_A + L_R + 12$$

using the initial estimate $c = 1$.

Compute η from

$$sc\left[\frac{nK_0 U}{K}\middle| 1 - m0\right] = \left[10 \uparrow \left(\frac{L_R}{10}\right) - 1\right]^{1/2}$$

and

$$\eta = sc\,[U \mid 1 - m]$$

using the conditional requirement

$$\frac{nK_0}{K} = \frac{K_0'}{K'}$$

then the resonant frequencies of the stubs occur when

$$\lambda_{gr} = \lambda_{gp} - (\lambda_{gp} - \lambda_{g2}) \left[\frac{1 - m^{1/2}C_r}{(1 + m^{1/2}cC_r)(1 + m^{1/2}(1 + c))}\right]$$

where

$$C_r = cd\left[\frac{(2r-1)K}{n}\right], \qquad r = 1 \rightarrow n$$

possess a 3-dB bandwidth

$$\Delta\lambda_{gr} = \frac{2\eta(1 - m)m^{1/2}(1 + c)S_r N_r}{(1 + m^{1/2}cC_r)(1 + m^{1/2}(1 + c))}, \qquad (\lambda_{gp} - \lambda_{g2})$$

$$\left(S_r = sd\left[\frac{(2r-1)K}{n}\right] \; N_r = nd\left[\frac{(2r-1)K}{n}\right]\right)$$

and are separated by the phase lengths

$$\psi_{r,r+1}\,|_{\lambda_g = \lambda_{gp}} = \cot^{-1}[\eta m^{1/2} sn[2rK/n]], \qquad r = 1 \rightarrow n - 1$$

with $(0 < \psi_{r,r+1} < \pi/2)$.

B. Quasi Low-Pass (Stub Separation $>\lambda_{gp}/2$, $<3\lambda_{gp}/4$)

The design equations are the same as in Section II-A apart from

$$\lambda_{gr} \rightarrow \lambda_{gr}\left(1 + \frac{3\sqrt{3}\pi}{4}\left(\frac{\Delta\lambda_{gr}}{\lambda_{gp}}\right)^2\right)$$

$$\psi_{r,r+1} \rightarrow \psi_{r,r+1} + \pi - \tan^{-1}\left(\frac{3\sqrt{3}\pi\Delta\lambda_{gr}}{4\lambda_{gp}}\right) - \tan^{-1}\left(\frac{3\sqrt{3}\pi\Delta\lambda_{gr+1}}{4\lambda_{gp}}\right)$$

and the susceptances of the capacitive discontinuities under the stubs at $\lambda_g = \lambda_{gp}$ are

$$B_r = \frac{3\sqrt{3}\pi\Delta\lambda_{gr}}{4\lambda_{g0}}.$$

C. Quasi High-Pass (Stub Separation $> \lambda_{gp}/4$, $<\lambda_{gp}/2$)

In this case $\lambda_{gp} < \lambda_{g2}$ and if λ_{g1} and λ_{g2} are interchanged, the design equations are the same as in Section II-A, taking the magnitude of the values for the bandwidths of the stubs, apart from

$$\psi_{r,r+1} = \pi - \psi_{r,r+1}.$$

We shall now establish these results commencing with the derivation of the basic prototype filter.

III-A. THE CHEBYSHEV SINGLE-SIZED PROTOTYPE

The low-pass prototype Chebyshev filter operating between 1-Ω terminations and using series inductors and impedance inverters possesses element values given by

$$L_r = \frac{2\sin[(2r-1)\pi/2n]}{\eta}, \qquad r = 1 \rightarrow n$$

and

$$K_{r,r+1} = \frac{\{\eta^2 + \sin^2[r\pi/n]\}^{1/2}}{\eta}, \qquad r = 1 \rightarrow n - 1 \quad (1)$$

where L_r is the inductance of the rth series element and $K_{r,r+1}$ is the characteristic impedance of the impedance inverter located between the rth and $(r + 1)$th series inductors.

The auxiliary parameter η is given by

$$\eta = \sinh\left[\frac{1}{n}\sinh^{-1}\frac{1}{\epsilon}\right] \quad (2)$$

where the passband $(|\omega| \leq 1)$ return loss has a minimum value

$$L_R = 10\log\left(1 + \frac{1}{\epsilon^2}\right) \quad (3)$$

and the insertion loss L_A at a frequency in the stopband $\omega' > 1$ is

$$L_A = 10\log[1 + \epsilon^2\cosh^2(n\cosh^{-1}\omega')]. \quad (4)$$

Consider the frequency transformation

$$\omega \rightarrow \left(1 + \cos\frac{\pi}{2n}\right)\omega - \cos\left(\frac{\pi}{2n}\right) \quad (5)$$

which results in the insertion loss characteristic shown in Fig. 3 with perfect transmission at the origin and a low-pass cutoff frequency of unity. The rth series element now possesses an impedance

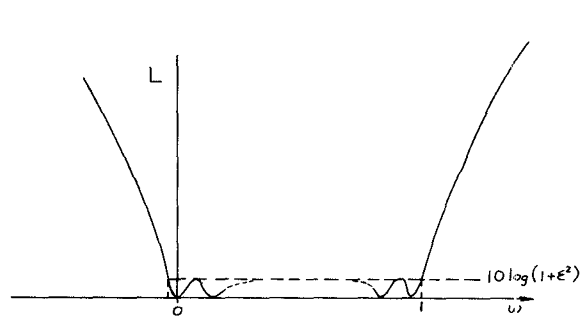

Fig. 3. Modified Chebyshev prototype insertion loss characteristic.

$$j\left[\frac{2\sin[(2r-1)\pi/2n]}{\eta}\right]\left[\left(1+\cos\frac{\pi}{2n}\right)\omega-\cos\frac{\pi}{2n}\right] \tag{6}$$

which is the series connection of an inductor

$$L_R' = \frac{2\sin[(2r-1)\pi/2n](1+\cos\pi/2n)}{\eta} \tag{7}$$

and a frequency invariant reactance [4] of value

$$jX_r = -j\frac{2}{\eta}\sin\left[\frac{(r-1)\pi}{2n}\right]\cos\frac{\pi}{2n} \tag{8}$$

which may be reduced to

$$jX_r = \frac{-j}{\eta}\left[\sin\left[\frac{(r-1)\pi}{n}\right]+\sin\left[\frac{r\pi}{n}\right]\right]. \tag{9}$$

Associating the first term with the preceding impedance inverter and the second with the following impedance inverter, the series inductors are therefore coupled by networks defined by the overall transfer matrix

$$\begin{bmatrix}1 & -j\frac{\sin(r\pi/n)}{\eta}\\ 0 & 1\end{bmatrix}\begin{bmatrix}0 & j\frac{[\eta^2+\sin^2(r\pi/n)]^{1/2}}{\eta}\\ j\frac{\eta}{[\eta^2+\sin^2(r\pi/n)]^{1/2}} & 0\end{bmatrix}\cdot\begin{bmatrix}1 & -j\frac{\sin(r\pi/n)}{\eta}\\ 0 & 1\end{bmatrix}$$

$$= [\eta^2+\sin^2(r\pi/n)]^{-1/2}\cdot\begin{bmatrix}\sin(r\pi/n) & j\ \eta\\ j\ \eta & \sin(r\pi/n)\end{bmatrix} \tag{10}$$

which is an ideal phase shifter with a transfer matrix

$$\begin{bmatrix}\cos\psi_{r,r+1} & j\sin\psi_{r,r+1}\\ j\sin\psi_{r,r+1} & \cos\psi_{r,r+1}\end{bmatrix} \tag{11}$$

with the phase shift

$$\psi_{r,r+1} = \tan^{-1}\left(\frac{\eta}{\sin(r\pi/n)}\right). \tag{12}$$

Thus the new prototype network possesses the equivalent circuit shown in Fig. 4 with the element values given by (7) and (12).

Consider the additional narrow-band bandstop frequency transformation

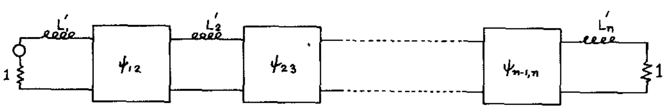

Fig. 4. Modified prototype network with resonators and ideal phase shifters.

$$\omega \rightarrow \frac{\omega(\omega_0-1)}{(\omega_0-\omega)} \tag{13}$$

where ω_0 is greater than, but close to, unity, i.e.,

$$\omega_0 = 1+b \qquad (b \text{ small}). \tag{14}$$

From (5) and (13), the argument of the Chebyshev polynomial will now be

$$\frac{(1+\cos[\pi/n]2)\omega(\omega_0-1)}{(\omega_0-\omega)} - \cos\left[\frac{\pi}{2n}\right] \tag{15}$$

and if ω_1 and ω_2 are two frequencies in the stopband where the insertion loss is the same we have

$$(1+c)(\omega_0-1)\left[\frac{\omega_1}{\omega_0-\omega_1}+\frac{\omega_2}{\omega_0-\omega_2}\right] = 2c \tag{16}$$

where

$$c = \cos\left(\frac{\pi}{2n}\right).$$

Now if $1 < \omega_1 < \omega_0 < \omega_2$ we may write

$$\omega_1 = 1+b(1-a), \qquad \omega_2 = 1+b(1+d) \tag{17a}$$

where

$$a = \frac{\omega_0-\omega_1}{\omega_0-1}$$

$$d = \frac{\omega_2-\omega_0}{\omega_0-1} \tag{17b}$$

and (16) reduces to

$$-2b+\frac{(d-a)(1+b)}{ad} = \frac{2c}{1+c} \tag{18a}$$

or

$$(1-a)(1+d)\approx 1, \qquad \text{if } \frac{b}{1+b}+c\approx\frac{1+c}{2}. \tag{18b}$$

Given the ratio of the stopband bandwidth $\omega_2-\omega_1$ to the guardband ω_1-1, it is necessary to determine the arguments of the Chebyshev polynomial at ω_1 in order to obtain the attenuation level for a given degree, i.e., obtain

$$y = \frac{(1+c)\omega_1(\omega_0-1)}{(\omega_0-\omega_1)} - C$$

$$= \frac{(1+c)(1+b(1-a))}{a} - C \tag{19}$$

given

$$x = \frac{(1-a)}{(a+d)} = \frac{\omega_1-1}{\omega_2-\omega_1}. \tag{20}$$

For b small, using (18), (19), and (20) we have

$$y = (1 + c)\{\tfrac{1}{2} + x + [x(1+x)]^{1/2}\}. \quad (21)$$

To illustrate the effect of this transformation consider the example where $\omega' = \frac{5}{3}$ for a specified attenuation in the low-pass prototype network. In our notation, $x = \frac{1}{3}$ and hence $y = (1 + c)\frac{3}{2}$, or in general, from (21) $y = \omega' + (\omega'^2 - 1)^{1/2}$.

If L_A is the stopband attenuation $\omega_1 < \omega < \omega_2$, and L_R is the minimum return loss for $\omega < 1$, then

$$L_A + L_R = 20n \log [y + (y^2 - 1)^{1/2}] \quad (22)$$

thus enablng the degree of the required network to be determined.

III-B. THE ELLIPTIC FUNCTION SINGLE-SIDED PROTOTYPE

In the "natural" low-pass prototype elliptic function filter [4], operating between 1-Ω terminations using series impedances Z_r separated by impedance inverters, we have

$$Z_r = j\left[\frac{2\eta(1-m)sd[(2r-1)K/n]nd[(2r-1)K/n]\omega}{1 - cd[(2r-1)K/n]\omega} - \eta m\left[sn\left[\frac{2(r-1)K}{n}\right] + sn\left[\frac{2rK}{n}\right]\right] \cdot cd\left[\frac{K}{n}\right]cd\left[\frac{(2r-1)K}{n}\right]\right], \quad r = 1 \to n \quad (23)$$

and

$$K_{r,r+1} = \{1 + \eta^2 m sn^2[2rK/n]\}^{1/2}, \quad r = 1 \to n-1 \quad (24)$$

with the elliptic functions defined as in [3] and [4] and

$$\eta = sc[U/1-m], \qquad \text{sc}\left[\frac{nK_0U}{K}\middle|\, 1-m_0\right] = \frac{1}{\epsilon} \quad (25)$$

with m and m_0 being related through the conditional requirement

$$\frac{nK_0}{K} = \frac{K_0'}{K'}. \quad (26)$$

In this case, the passband occurs for $|\omega| \leq m^{1/2}$ with a minimum return loss $L_R = 10 \log (1 + \epsilon^2/m_0)$ and the stopband for $|\omega| > 1$ with a minimum insertion loss of $L_A = 10 \log (1 + 1/\epsilon^2)$.

Consider the frequency transformation

$$\omega \to m^{1/2}\left[\frac{(1 + cd[K/n])\omega}{1 + (1-\omega)m^{1/2}(1 + cd[K/n])} - cd[K/n]\right] \quad (27)$$

which produces the insertion loss characteristic depicted in Fig. 5, where the cutoff frequency for the stopband is

$$\omega_c = \frac{(1 + m^{1/2}c)(1 + m^{1/2}(1+c))}{m^{1/2}(1+c)(2 + m^{1/2}c)}, \qquad (c = cd[K/n]). \quad (28)$$

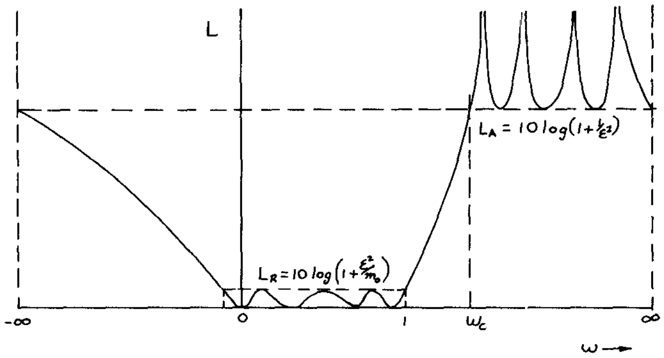

Fig. 5. Modified elliptic function prototype.

Proceeding in a manner similar to the Chebyshev case, results in a new prototype network with series impedances given by

$$Z_r' = j\eta\left[\frac{2(1-m)sd[(2r-1)K/n]nd[(2r-1)K/n]\omega}{1 + (1 + m^{1/2}c)cd[(2r-1)K/n](\omega - \omega_r)} - m^{1/2}\left[sn\left[\frac{2(r-1)K}{n}\right] + sn\left[\frac{2rK}{n}\right]\right]\right] \quad (29)$$

where

$$\omega_r = \frac{(1 + m^{1/2}c cd[(2r-1)K/n])(1 + m^{1/2}(1+c))}{m^{1/2}(1+c)[1 + (1 + m^{1/2}c)cd[(2r-1)K/n]]} \quad (30)$$

separated by impedance inverters of characteristic impedance

$$K_{r,r+1} = \{1 + \eta^2 m sn^2[2rK/n]\}^{1/2}. \quad (31)$$

Alternately, this may be expressed as series elements with series impedances

$$j\frac{A_r\omega}{\omega - \omega_r} \quad (32)$$

with

$$A_r' = \frac{2\eta(1-m)sd[(2r-1)K/n]nd[(2r-1)K/n]}{[1 + (1 + m^{1/2}c)cd[(2r-1)K/n]]} \quad (33)$$

and ω_r given by (30), separated by ideal phase shifters of phase length

$$\psi_{r,r+1} = \cot^{-1}[\eta m^{1/2} sn[2rK/n]]. \quad (34)$$

Applying a frequency transformation similar to (13), i.e.,

$$\omega \to \frac{\omega(\omega_2 - 1)}{(\omega_2 - \omega)} \quad (35)$$

where ω_2 is the upper cutoff frequency of the stopband, yields

$$\frac{\omega_1(\omega_2 - 1)}{(\omega_2 - \omega_1)} = \frac{(1 + m^{1/2}c)(1 + m^{1/2}(1+c))}{m^{1/2}(1+c)(2 + m^{1/2}c)} = 1 + x \quad (36)$$

where x is the ratio of the guardband to stopband bandwidth, i.e.,

$$x = \frac{1 - m^{1/2}}{m^{1/2}(1 + c)(2 + m^{1/2}c)} \tag{37}$$

or

$$m^{-1/2} = \frac{1 + (1 + c)x + [1 + 4(1 + c)^2 x + 4(1 + c)^2 x^2]^{1/2}}{2}. \tag{38}$$

Furthermore we have [3]

$$\Delta B_r = \frac{2 \sin [(2r - 1)\pi/2n](y + \cos \pi/2n)(1 + \cos \pi/2n)(f_1 - f_0)}{\eta(y - 1)} \tag{43}$$

$$L_A + L_R = 13.65 \cdot \frac{nK'}{K} - 12 \tag{39}$$

and using (38) and (39), the degree of the network required to meet a given specification may be obtained.

IV. THE WAVEGUIDE SINGLE-SIDED FILTER

A. Quasi Low-Pass (Stub Separation $< \lambda_{gp}/4$*)*

The basic physical structure which is used to produce the single passband and stopband requirements is illustrated in Fig. 1 where the series stubs are iris-coupled rectangular resonators. However, in order that any form of series resonator may be used, the basic design equations

$$x_r = \frac{1 - m^{1/2} cd[(2r - 1)K/n]}{(1 + m^{1/2} cd[K/n] cd[(2r - 1)K/n])(1 + m^{1/2}(1 + cd[K/n]))} \tag{46}$$

$$\Delta\lambda_{gr} = \frac{2\eta(1 - m) sd[(2r - 1)K/n] nd[(2r - 1)K/n] m^{1/2}(1 + cd[K/n])(\lambda_{gp} - \lambda_{g2})}{(1 + m^{1/2}(1 + cd[K/n]))(1 + m^{1/2} cd[K/n] cd[(2r - 1)K/n])}, \tag{47}$$

are developed in terms of quantities related to the main guide wavelength λ_g and impedance (normalized to unity), and the resonators are uniquely defined by their resonant frequencies and 3-dB (or 20-dB) bandwidth. Normally, the design engineer would choose the elliptic function prototype since the final filter is physically similar to the Chebyshev case but fewer elements will be required. However, for very narrow bandwidths or large stopband levels, the Chebyshev prototype may be preferred due to dissipation loss in the resonators deteriorating the stopband behavior.

Using the information in the previous sections, the degree of the required filter may be obtained where the ratio of stopband to guardband bandwidth is

$$x = \frac{\lambda_{gp} - \lambda_{g1}}{\lambda_{g1} - \lambda_{g2}}. \tag{40}$$

Initially, we shall consider the Chebyshev prototype. Consequently, the final frequency transformation (13) as applied to the prototype shown in Fig. 4 is modified to

$$\omega \to \frac{(\lambda_{gp} - \lambda_{g0})}{(\lambda_g - \lambda_{g0})} \tag{41}$$

where, from (18) and (21)

$$\lambda_{g0} = \lambda_{g1} - (\lambda_{gp} - \lambda_{g1})\left(\frac{1 + c}{y - 1}\right). \tag{42}$$

Furthermore, using (7), the 3-dB bandwidth of the rth resonator is (43) and since the phase length between resonators is most sensitive around the passband edge, we equate these to lengths of waveguide at $\lambda_g = \lambda_{gp}$. Thus the basic design equations follow immediately.

For the elliptic function case, the transformation (35) becomes

$$\omega \to \frac{(\lambda_{gp} - \lambda_{g2})}{(\lambda_g - \lambda_{g2})} \tag{44}$$

and following a similar approach as used in the Chebyshev case

$$\lambda_{gr} = \lambda_{gp} - (\lambda_{gp} - \lambda_{g2}) x_r \tag{45}$$

with (46), (47), and

$$\psi_{r,r+1}|_{\lambda_g = \lambda_{gp}} = \cot^{-1} [\eta m^{1/2} sn[2rK/n]] \tag{48}$$

resulting in the basic design equations given in Section II.

B. Quasi Low-Pass (Stub Separation $> \lambda_{gp}/2, < 3\lambda_{gp}/4$*)*

With the desirable restriction of using essentially a uniform guide without stepped impedance discontinuities, a technique must be obtained to reduce the passband attenuation at low frequencies due to the effect described in the Introduction. Since changing the impedance of the stubs will not affect the deterioration of the response when the phase separation of the stubs is of the order of π radians additional elements must be added. The simplest is a capacitive discontinuity in the broad wall of the waveguide on the opposite side to each stub which may take the form of a tuning screw. This represents neither a simple series nor shunt connection as the equivalent circuit will take the form of a lattice.

Since we are at liberty to modify the length of the guide separating the stubs the basic section which we must consider is shown in Fig. 6. To a first approximation, we may represent the series resonator by the impedance

$$jZ \tan\theta = j\frac{\pi}{2}\frac{\lambda_{g0}'}{\lambda_g}Z \tag{49}$$

the electrical length of line by

$$\psi = a\frac{\lambda_{gp}}{\lambda_g} \tag{50}$$

and for the capacitive discontinuity

$$jB = jB_p\frac{\lambda_{gp}}{\lambda_g}. \tag{51}$$

Forming the even- and odd-mode impedances

$$Z_e = \frac{-j(1 - \frac{1}{2}B\tan\psi)}{(\tan\psi + \frac{1}{2}B)} \tag{52}$$

and

$$Z_0 = \frac{j(\frac{1}{2}Z\tan\theta + \tan\psi)}{(1 - \frac{1}{2}Z\tan\theta\tan\psi)}. \tag{53}$$

For λ_g in the vicinity of λ_{gp}, this section must approximate to a series stub, i.e., $Z_e = \infty$, yielding

$$\tan a = \frac{-B_p}{2} \tag{54}$$

and Z_0 must resonate at $\lambda_g = \lambda_{g0}$, i.e.,

$$1 + \frac{Z}{\pi(1 - \lambda_{g0}'/\lambda_{g0})}\frac{B_p}{2} = 0$$

or

$$\lambda_{g0'} = \lambda_{g0}\left(1 + \frac{ZB_p}{2\pi}\right) \tag{55}$$

and from (53), the impedance of the stub is still approximately Z.

Finally, we require the section to be all-pass at a lower frequency defined by $\lambda_{ga} > \lambda_{gp}$ with λ_{ga} probably of the order of $\frac{3}{2}\lambda_{gp}$. For the all-pass condition we require

$$1 - Z_eZ_0 = 0 \tag{56}$$

and for Z small, substituting (52) and (53) into (56)

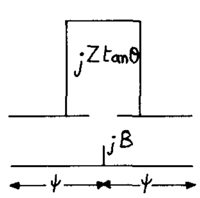

Fig. 6. Basic resonator section with capacitive discontinuity symmetrically embedded in a negative length of guide.

gives

$$B_p = Z\frac{\lambda_{ga}}{\lambda_{gp}}\tan\left(\frac{\pi}{2}\frac{\lambda_{g0}'}{\lambda_{ga}}\right). \tag{57}$$

In the specific case of $\lambda_{ga} = \frac{3}{2}\lambda_{gp} \approx \frac{3}{2}\lambda_{g0}'$

$$B_p = \frac{3\sqrt{3}}{2}Z \tag{58}$$

yeilding the specific design equations cited.

It should be noted that the introduction of the capacitive discontinuities can be accomplished using tuning screws as can the modification to the resonant frequency of the stubs. Thus the only change mechanically is the distance between the stubs. If this is not corrected then a lower passband ripple (higher return loss) will result at the expense of a loss in selectivity and reduction in the bandwidth of the stopband since this process can be compensated for by a change in the value of η (see design equations).

C. Quasi High Pass (Stub Separation $>\lambda_{gp}/4$, $<\lambda_{gp}/2$)

The results for the quasi high-pass response are obtainable directly from the low-pass prototype after the substitution $\omega \rightarrow -\omega$, $\eta \rightarrow -\eta$.

V. COMPUTER SIMULATION OF THE SINGLE-SIDED WAVEGUIDE FILTERS

Simulated results were computed for the cases of Sections IV-A, B, and C. In the former two cases the prescribed specification was

waveguide WR90
stopband 10 → 10.2 GHz, $L_A > 40$ dB
passband < 9.95 GHz $L_R > 26$ dB

and for case C,

passband > 10.25 GHz, $L_R > 26$ dB.

On a Chebyshev basis, the number of cavities required is 5 and the results are plotted in Fig. 7. In all cases, there was a slight reduction in the return loss in the passband accompanied by a corresponding increase in the insertion loss in the stopband. Due to the frequency dependence of the guide coupling the stubs, the passband exhibits a deterioration remote from the stopband.

VI. EXPERIMENTAL RESULTS

The filter cited in Section IV-B above was constructed and tested.

Initially, no capacitive discontinuities were introduced to illustrate the effect of the frequency dependence of the coupling lines. The results on return loss and insertion loss are shown in Fig. 8 showing that the passband has essentially been reduced to 200-MHz bandwidth. Introducing the capacitive tuning screws results in the significant increase in passband bandwidth as shown in Fig. 9.

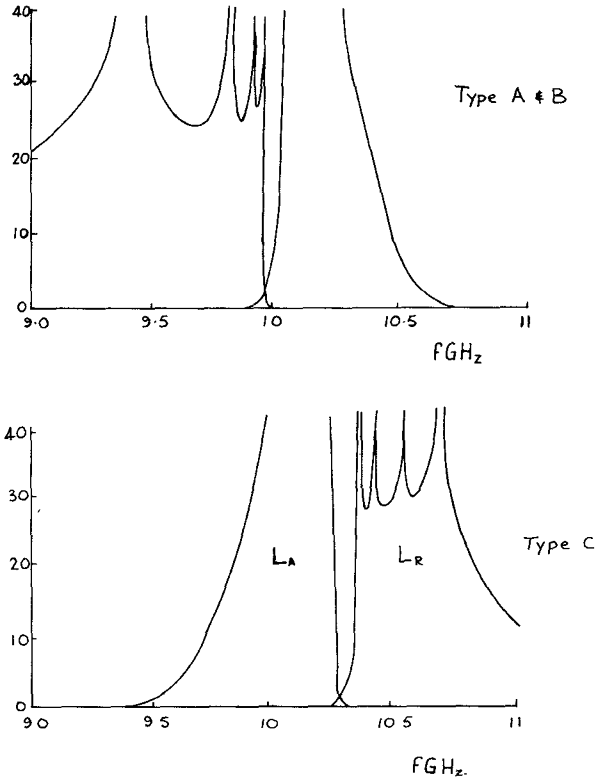

Fig. 7. Computed results for insertion loss and return loss for cases of Sections IV-A, B, and C.

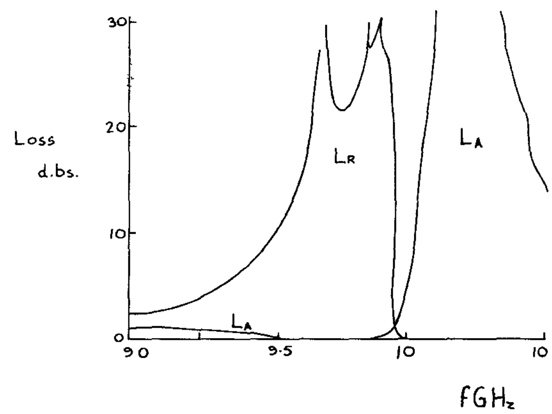

Fig. 8. Experimental results on fifth-degree X-band filter without capacitive compensation.

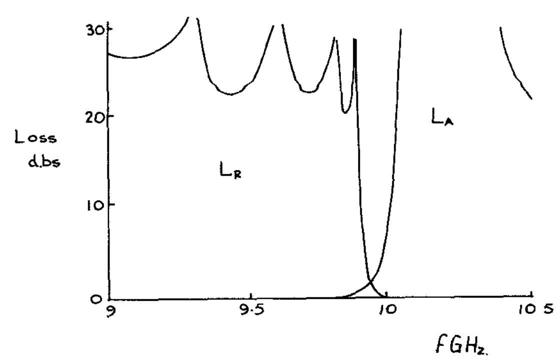

Fig. 9. Experimental results on fifth-degree X-band filter with capacitive compensation.

VII. CONCLUSIONS

Complete design formulas have been obtained for waveguide single-sided filters where only one passband and one stopband are required. It has been shown, that a significant reduction in the number of cavities needed to meet this type of specification can be obtained over conventional techniques. Furthermore, the structure is physically no more complicated than the conventional waveguide bandstop filter, the only difference being irregular spacings of the stubs.

The three classes of filters which achieve quasi low-pass or quasi high-pass responses have been discussed in detail and simulated on a digital computer. Finally, experimental results on a fifth-degree X-band filter have been presented for the three quarter wave coupled case with and without compensating capacitive discontinuities showing very close agreement to theoretical predictions.

REFERENCES

[1] S. B. Cohn, "Direct-coupled-resonator filters," *Proc. IRE*, vol. 45, pp. 187–196, Feb. 1957.
[2] G. L. Matthaei, L. Young, and E. M. T. Jones, *Microwave Filters, Impedance-Matching and Coupling Structures*. New York: McGraw-Hill, 1964.
[3] J. D. Rhodes, "Waveguide bandstop elliptic function filters," *IEEE Trans. Microwave Theory Tech.*, vol. MTT-20, pp. 715–718, Nov. 1972.
[4] ——, "Explicit formulas for element values in elliptic function prototype networks," *IEEE Trans. Circuit Theory*, vol. CT-18, pp. 264–276, Mar. 1971.

Temperature-Stabilized 1.7-GHz Broad-Band Lumped-Element Circulator

HIDEHIKO KATOH

***Abstract*—A new construction technique for broad-banding and temperature stabilization of a lumped-element circulator is presented to obtain a compact circulator for practical usage. By using a new integrated wide-banding network consisting of three series resonant circuits on the back of the junction substrate, 1.7-GHz double-tuned and triple-tuned broad-band circulators have been successfully developed. Fundamental junction parameters, such as an in-phase eigeninductance, parasitic capacitance, and nonreciprocal filling factor, have been investigated experimentally.**

A design theory for temperature compensation of a lumped-element circulator is also presented, and temperature compensation with bias magnetic field of postitive temperature coefficient has been applied to the 1.7-GHz broad-band circulators. As a result, 20-dB isolation bandwidths of more than 600 MHz (double-tuned type) and 950 MHz (triple-tuned type) have been obtained throughout the temperature range of $-10 \sim +60°C$.

I. INTRODUCTION

RECENT PROGRESS of thin-film lumped-element microwave integrated circuits (IC) for lower microwave frequencies has stimulated the need for miniaturized nonreciprocal circuits which are well adapted to the integrated circuits. By applying microwave IC technology, Knerr [1] realized an L-band lumped-element circulator [2], and afterwards achieved a 20-dB isolation relative bandwidth of more than 30 percent by inserting a capacitor between the junction base conductor and ground [3]. This broad-banding technique was recognized later [4] to be equivalent with the one proposed by Konishi and Hoshino [5], in which the in-phase eigenvalue is excited by an explicit resonant circuit. It is expected from the analysis by Konishi and Hoshino [5] that a broader bandwidth can be obtained if the resonant circuit is properly optimized. However, no experimental investigation in this respect has been made so far for frequency bands above 1.0 GHz.

Therefore, the main purpose of this paper is to propose a lumped-element circulator construction that uses a new type of integrated wide-banding network which is optimally adjusted and suitable for microwave frequencies. Experimental results on circulator junction in regard to its eigeninductances, parasitic reactances, and nonreciprocal filling factor [6] are also described.

In addition to broad-banding, temperature stabilization is important from the practical point of view. Konishi [2] discussed temperature dependence of lumped-element circulator characteristics, but the result is not applicable at least to below resonance circulators. Thus another purpose of this paper is to present a temperature stabilization technique. A design theory for temperature compensation of a lumped-element circulator is derived, and a stabilization method using a bias magnetic field of a positive temperature coefficient is proposed.

Manuscript received August 5, 1974; revised February 3, 1975.
The author is with the Central Research Laboratories, Nippon Electric Co., Ltd., Nakahara-ku, Kawasaki, Japan.